Proceedings of ASME Turbo Expo 2011
GT2011
June 6-10, 2011, Vancouver, British Columbia, Canada

GT2011-45730

A STUDY OF STEAM-COOLED HUMIDIFIED GAS TURBINE CYCLES

Ching-Jen (CJ) Tang
GE Global Research
Energy Systems Lab
Niskayuna, NY, USA

ABSTRACT

Humidified Gas Turbine (HGT) cycles such as the Evaporative Gas Turbine (EGT) and the Steam-Injected Gas Turbine (STIG) using humid air as the working medium do not require a complete steam turbine bottoming cycle; thus, their initial capital costs are not as high as those for the conventional combined cycles. The performance of a HGT cycle could be comparable to a state-of-the-art combined cycle for small loads. The availability of the steam from a HGT cycle presents opportunities for designing steam-cooled blades. Since the specific heat capacity for steam is higher than that for air, steam could potentially be a better coolant for turbine blades than air, resulting in higher cycle efficiency.

In this study, three known HGT cycles are evaluated in terms of their electrical efficiencies and power outputs: the STIG, the Part-flow Evaporative Gas Turbine (PEvGT), and the combined STIG cycles. All the three HGT cycles are analyzed in two cooling options: steam and air coolings. The HGT cycles will be evaluated using consistent thermodynamic properties and assumptions. Like a simple gas turbine cycle, the HGT cycles are based on the well-known Brayton cycle whose performance is dictated by the cycle pressure ratio and turbine inlet temperature. Therefore, the electrical efficiencies and power outputs of the HGT cycles will be calculated as a function of the cycle pressure ratio and turbine inlet temperature.

The steam-cooled cycles provide advantages over the air-cooled cycles in the electrical efficiency, power output, and combustion stability. The steam cooling improves the electrical efficiency by approximately 1.4 percentage points for the STIG cycle, by approximately 1.7 percentage points for the PEvGT cycle, and by approximately 1 percentage point for the combined STIG cycle. The maximum electrical efficiency of the steam-cooled PEvGT cycle is 54.6%, only 0.2 percentage points higher than that for the steam-cooled combined STIG cycle. The steam cooling generally results in more power output than the air cooling does for all the HGT cycles at most operating conditions. In addition, the steam cooling reduces the water content of the humid air entering the combustor, leading to significantly improved combustion stability.

INTRODUCTION

Humidified Gas Turbine (HGT) cycles utilize humidified air as the working fluid expanding through the turbine expander to increase the thermal efficiency and specific power output over the simple gas turbine cycle. The HGT cycles include two main groups: Steam Injection Gas Turbine (STIG) and Evaporative Gas Turbine (EGT) cycles. Johsson and Yan [1] published a comprehensive review on the history and performance of various HGT cycles. Bhargava et al. [2] reviewed various STIG and EGT cycles with intercooled compressors. The basic STIG cycles have been extensively studied and been used commercially, such as Allison 501-KH [3], GE LM5000, and LM2500 STIG gas turbines [4]. Although many variations of the EGT cycles [5,6,7,8,9] have been published and studied, they remain at the demonstration stage. One of the most promising variations is the Part-flow Evaporative Gas Turbine (PEvGT) cycle [5]. Another variation of the EGT cycle is the Advanced Humid Air Turbine [7,8] (AHAT) developed by Hitachi. Araki et al. [8] published an electrical efficiency of 52.8% without a WAC (water atomization cooling) at a TIT of 1350ºC, ~1.8 percentage points higher than that published by Bartlett and Westermark [5]. Wang et al. [9] published their study for the Humid Air Turbine (HAT) cycle with an intercooled compressor and their results show an electrical efficiency of 50.6% at a TIT of 1200ºC, consistent with the results published by Bartlett [10]. Bhargava et al. [11] published an electrical efficiency of 56% for the intercooled HAT cycle with the most advanced technologies. The TIT for the HAT cycle is 1500ºC. The efficiency of the intercooled HAT is ~1 percentage point higher than that published by Bartlett [10].

The basic STIG cycle includes two main components: a gas turbine and a Heat Recovery Steam Generator (HRSG). The HRSG generates steam using the heat from turbine exhaust gas and the steam is injected back into the gas turbine to increase the power output and electrical efficiency. The STIG cycle offers more operating flexibility than the simple gas turbine cycle does. The GE LMS100 STIG with an intercooled compressor [12] shows an electrical efficiency of ~50%. One very popular variation of the STIG cycle is the Cheng cycle [3]. There are over 200 Cheng cycle systems operating around the world. Another variation for the STIG cycle is the combined STIG cycle [13,14]. The combined STIG cycle including a steam turbine has a higher efficiency than the STIG cycle.

The PEvGT cycle has been investigated and described in several references [5,6,10]. The main goal of the cycle is to reduce the heat transfer area and the pressure drops associated with the recuperative heat exchangers for the EGT cycle while achieving the same or higher electrical efficiency. Bartlett and Westermark [5] show that the electrical efficiency for the PEvGT cycle could be better than that for the EGT cycle.

A blade cooling system can significantly affect the overall performance of a gas turbine. Two well-known cooling systems include closed-loop convective cooling and open-loop film cooling. The coolant leaving turbine blades is often used to drive an intermediate-pressure steam turbine for the closed-loop system while the coolant is discharged into the mainstream through film holes for the open-loop system. Air and steam are the most popular coolants for turbine blade cooling. Most gas turbines are air-cooled and few gas turbines are steam-cooled. The GE H-class gas turbine based combined cycle uses closed-loop steam cooling system to raise electrical efficiency to 60%. This study focuses on an open-loop steam cooling system because of the simplicity of the open-loop steam cooling. In this study, steam and air-cooled HGT cycles are evaluated for the electrical efficiency and power output.

Although many studies have been published to evaluate the performances of various HGT cycles, it is rare to find studies addressing the PEvGT and combined STIG cycles using steam as a blade coolant. Additionally, it is very difficult to find articles directly comparing the combined STIG to PEvGT cycle using consistent assumptions.

In this study, three HGT cycles (STIG, combined STIG, and PEvGT) are evaluated using consistent thermodynamic properties and assumptions. Each HGT cycle has two options: steam and air coolings. Each HGT cycle is evaluated at various turbine pressure ratios and Turbine Inlet Temperatures (TIT's). In addition to the turbine pressure ratios and TIT's, the combined STIG is optimized for the highest electrical efficiency by varying the pressure of steam entering the steam turbine.

THE HGT CYCLES FOR ANALYSIS

The basic STIG cycle

Figure 1 shows a schematic of the basic STIG cycle with steam injected into the combustor or at the compressor exit. The feed water is heated into super-heated steam in the HRSG where the turbine exhaust gas is cooled down. The HRSG includes an economizer (Econ), evaporator (Evap), and super heater (SH). The HRSG is operated at one pressure determined by the evaporator. The one-pressure HRSG typically cannot recover low-quality heat from the turbine exhaust gas and has low second-law efficiency for heat recovery.

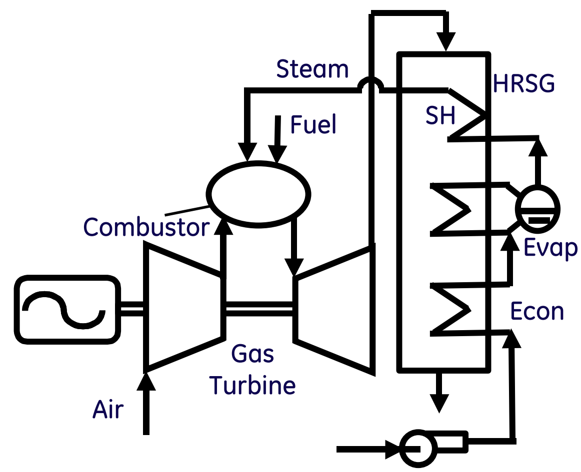

Figure 1. The schematic of the STIG cycle

The combined STIG cycle

The combined STIG cycle as shown in Figure 2 was described in several references [13,14]. This cycle includes a gas turbine, steam turbine, and two-pressure HRSG. The high-pressure steam from the HRSG expands through a steam turbine before injected into the combustor or the compressed air at the exit of the compressor. The low-pressure steam from the HRSG is directly injected into the combustor or the compressed air at the exit of the compressor. The two-pressure HRSG has a higher second-law efficiency than the one-pressure HRSG.

The PEvGT cycle

Figure 3 shows the concept of the PEvGT cycle [5] including a HRSG, a gas turbine, and a humidification tower. The humidification tower combined with the economizer is used to recover the low-grade heat from the turbine exhaust gas. The HRSG is used to raise the super-heated steam and heat up the humidified air injected into the combustor. The gas turbine has an extraction port at the exit of the compressor, where a portion of the compressed air is extracted, humidified, reheated, and injected to the combustor. The super-heated steam produced by the HRSG is injected into the humidified air entering the recuperative heat exchanger.

Bartlett and Westermark [5] studied the performance of the PEvGT cycle with varying the amount of the air extracted from the main compressed air. The increase of the ratio of the extraction air to main air increases the power output of the PEvGT cycle. However, the increase in the power output becomes marginal at high part-flow ratios. The electrical efficiency for the PEvGT cycle with a pressure ratio of 35 bar reaches the maximum at a part-flow ratio of 20%. In this study, the part-flow ratio is fixed at 20% for all the operation conditions.

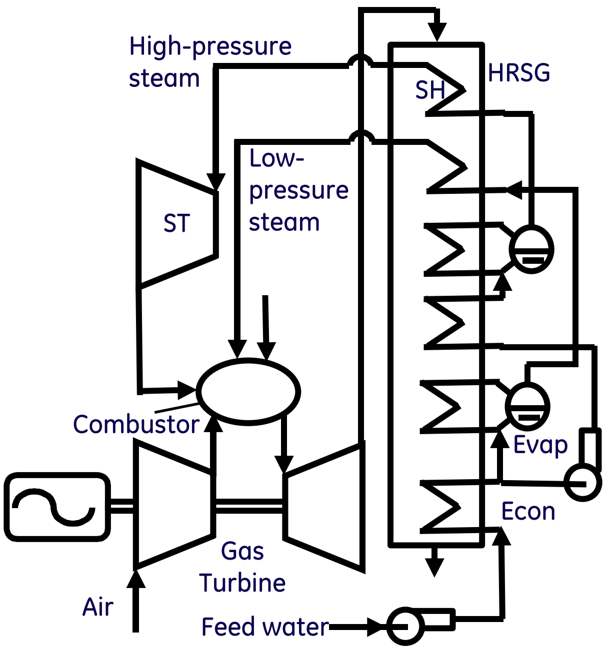

Figure 2. The schematic of the combined STIG cycle

Blade cooling

To simulate the effect of blade cooling on HGT performance, it is assumed that the stator and rotor rows of the first stage and the stator row of the second stage are film-cooled for all the HGT cycles. For film-cooled blades, cooling air or steam is discharged into the main hot gas path through the holes of the blade surface to form a cooling film.

To understand the impact of the cooling flow on the performance of a gas turbine, it is necessary to estimate the cooling flow. Holland and Thake [15] estimated the cooling air as a fraction of the air flow entering the compressor. Elmasri and Pourkey [16] estimated the cooling flow based on a semi-empirical cooling effectiveness relation below.

$$\frac{n_c \cdot c_{p,c}}{n_{gas} \cdot c_{p,gas}} = CF \cdot ARC \cdot \left(\frac{\varphi_\infty}{\varphi_\infty - \varphi} \right)^\beta \qquad (1)$$

$$\varphi = \frac{T_{gas} - T_{blade}}{T_{gas} - T_{coolant}} \qquad (2)$$

Equations (1) and (2) are used to calculate the coolant flow rates in this study. The maximum cooling effectiveness, φ_∞, is the asymptotic value at infinitely high coolant flow rates. φ_∞ suggested for the film cooling is 1.0 [16]. *ARC* is 0.05 and β is 0.9 in this study. The Correction Factor, CF, is used to account for the thermal barrier coating on the surfaces of the blades.

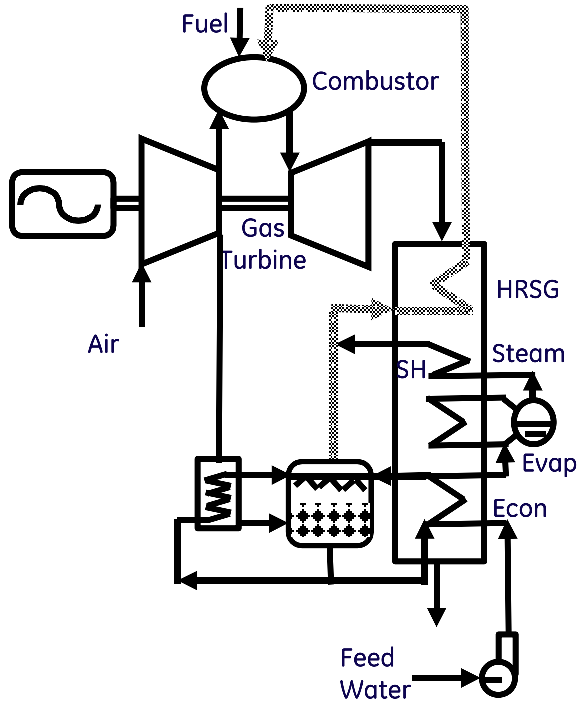

Figure 3. The schematic of the PEvGT cycle

Cycle modeling

All the HGT cycles were simulated by Thermoflex and Microsoft Excel. To compare all the HGT cycles, it is assumed that the technologies for the key components are the same. This implies that the turbine uncooled stage efficiency and the maximum allowable metal temperatures are the same. The baseline assumptions for this analysis are described below.

Gas turbine engine

In this study the turbine engines are specially designed for the three different HGT cycles such that the expanders can efficiently expand the compressed air and additional steam and such that the pressure loss for injecting steam or humid air to the combustor is minimized. The turbine engines share the same performances of the key features, as shown in Table 1. The compressor is designed to deliver ~124 kg/s (273 lb/s) compressed air at the ISO conditions while the turbine expander is sized for additional moisture depending on each HGT cycle. The compressor is not intercooled and its polytropic efficiency is 89%. The turbine expander has three stages and the stator and rotor rows of the first stage and the stator row of the second stage are cooled by air or steam. The uncooled efficiencies of the first two stages are 92% and the efficiency of the third stage is 90%. In the analysis, it is assumed that the combustion stability for these HGT cycles is always established at all the operating conditions. The design metal temperatures of the first and second stage stators are 832°C (1530°F) while the design metal temperature of the first stage rotor is 816°C (1500°F).

Steam turbine and HRSG

Table 2 shows key assumptions for the HRSG and the steam turbine for the combined STIG cycle. The steam turbine for the combined STIG cycle has a step efficiency of 86% and a pressure ratio of 1.35 for each step. The pinch temperature difference of the evaporator is 11.1°C (20°F) for the HGT cycles analyzed in this study.

Table 1 Gas turbine characteristics

Compressor	
Compressor inlet flow	124 kg/s
Compressor polytropic efficiency	89%
Combustor	
Δp/p across combustor	3.85%
Gas turbine	
Number of stages	3
Uncooled isentropic efficiency of 1st stage	92%
1st stage stator metal temperature	832°C
1st stage rotor metal temperature	816°C
Uncooled isentropic efficiency of 2nd stage	92%
2nd stage stator metal temperature	832°C
Isentropic efficiency of 3rd stage	90%

Table 2. Steam Turbine and HRSG

	STIG	PEvGT	Combined STIG
Steam turbine step efficiency	NA	NA	86%
1st evaporator pinch temperature difference	11°C	11°C	11°C
2nd evaporator pinch temperature difference	NA	NA	11°C

Key pressure losses

Table 3 shows the key pressure losses for the three HGT cycles. These pressure losses significantly affect the power output and efficiency of the three HGT cycles. The pressure loss caused by injecting steam into the combustor is assumed to be 10.3 bar (150 psi) for both the STIG and combined STIG cycles. This pressure loss based on specially designed STIG gas turbines is likely lower than those for commercially available STIG turbines with retrofitted injection ports. The pressure loss due to the humidification process is assumed to be 2.76 bar (40 psi) for the PEvGT cycle. This pressure loss includes the losses associated with air extraction from the compressor exit, with the recuperative heat exchanger, and with air re-entering the main flow. The pressure loss on the flue gas side of the HRSG is assumed to be ~1.4 kPa (0.2 psi) for the three HGT cycles. The HRSG includes an economizer, evaporator(s), and superheater(s) for the STIG and combined STIG cycles. In additional to these three HRSG components, the HRSG for the PEvGT cycle also includes a recuperative heat exchanger used to heat the humidified air up to a desired temperature.

Table 3. The key pressure losses

	STIG	PEvGT	Combined STIG
Steam injection, bar	10.3	NA	10.3
Humidification process including air flow extracted from turbine and humidified air flow heated up in recuperator and re-entering turbine, bar	NA	2.76	NA
Flue gas side of HRSG, kPa	1.4	1.4	1.4

Parametric study

Table 4 shows three variables and their values for this parametric study. The TIT and pressure ratio across the turbine expander are two key parameters determining the performance of a turbine engine. This study investigates the effect of the TIT and pressure ratio on the power outputs and efficiencies of the three HGT cycles. It is assumed that the compressor can operate without intercooling for all the cycles in the analysis. In addition to the TIT and pressure ratio, the pressure of the steam entering the steam turbine could affect the performance of the combined STIG cycle. The cycle performances at various steam pressures are calculated to determine an optimal steam pressure for the maximum efficiency of the combined STIG cycle.

Table 4. The variables for parametric study

Variable	Values
Turbine inlet temperature,°C	1260, 1371, 1482
Turbine pressure ratio	16 – 40
Pressure of steam entering steam turbine for combined STIG, bar	86 –134

RESULTS AND DISCUSSION

To investigate the performances of the three HGT cycles, the power output versus the electrical efficiency plots (performance map) are constructed at three different TIT's and various pressure ratios of the turbine expander as shown in Table 4.

Figure 4 shows three solid curves for the steam-cooled STIG cycle and three dotted curves for the air-cooled STIG cycle. As the TIT increases from 1260 to 1482°C (2300 to 2700°F) for the air-cooled STIG cycle, the power output increases ~34 MW and the electrical efficiency gains ~1.9 percentage points at a turbine pressure ratio of 16. The increase of the TIT results in a longer expansion line for the turbine expander and in a higher turbine exhaust gas temperature, leading to more power output. The increase of the TIT also implies a higher heat addition temperature, resulting in a higher electrical efficiency. The increase of the pressure ratio reduces the power output but increases the efficiency initially. Since the increase of the pressure ratio reduces the amount of the heat added to the cycle, the power output is reduced. The optimal pressure ratio for the maximum efficiency slightly increases with an increase in the TIT's. The optimal efficiency occurs at a pressure ratio between 25 and 28 for a TIT between 1260 and 1482°C.

At a given pressure ratio, the electrical efficiency for the steam-cooled STIG cycle is in general higher than that for the air-cooled STIG cycle, except for the pressure ratio of 16. The maximum electrical efficiency for the steam-cooled cycle with a TIT of 1482°C is 53.5%, 1.4 percentage points higher than that for the air-cooled cycle. The increase of the pressure ratio increases the advantage of the steam-cooled cycle over the air-cooled cycle in the electrical efficiency because the increase of the pressure ratio increases the difference between the required cooling flows for the air-cooled and steam-cooled cycles. The required amount of cooling flow strongly depends on the temperature of the cooling flow. As the pressure ratio increases, the temperature of the cooling air increases significantly but the temperature of the cooling steam stays roughly the same.

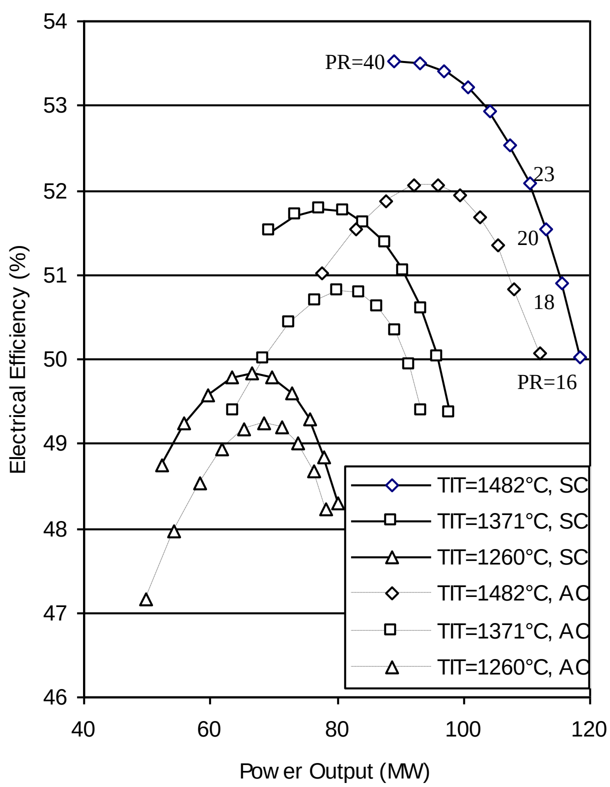

Figure 4. Electrical efficiencies and power outputs of steam and air-cooled STIG cycles.

Figure 5 shows three solid and dotted curves for the steam- and the air-cooled PEvGT cycles. As the TIT increases from 1260 to 1482°C for the air-cooled PEvGT cycle, the power output adds 25 MW and the electrical efficiency gains 1.8 percentage points for a pressure ratio of 16. These trends are the same as those for the STIG cycles. The increase of the pressure ratio reduces the power output but initially increases the efficiency for the air-cooled PEvGT cycle. The optimal pressure ratio for the maximum efficiency slightly increases with an increase in the TIT's. The optimal efficiency for a TIT's between 1482 and 1260°C occurs at a pressure ratio between 31 and 28.

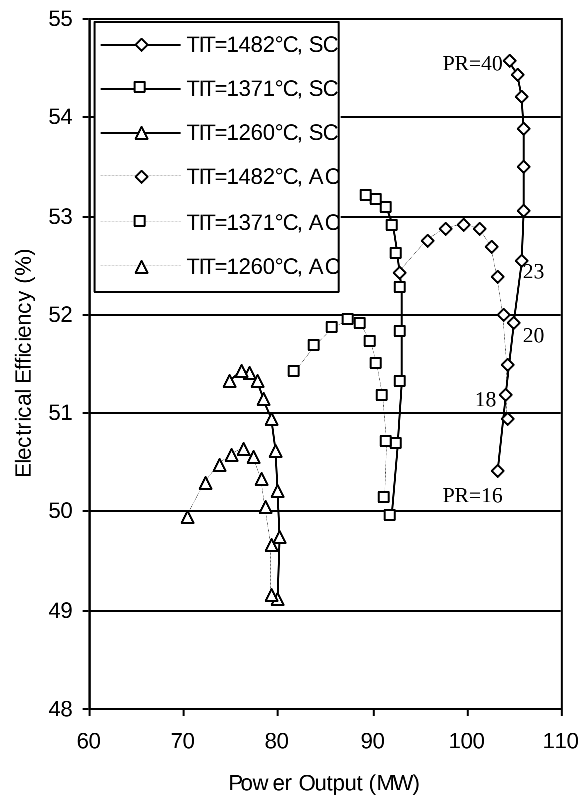

Figure 5. Electrical efficiencies and power outputs of steam and air-cooled PEvGT cycles.

At a given pressure ratio, the electrical efficiency for the steam-cooled PEvGT cycle is in general higher than that for the air-cooled PEvGT cycle, except for pressure ratios below 20. The maximum electrical efficiency for steam-cooled cycle with a TIT of 1482°C is 54.6%, 1.6 percentage points higher than that for the air-cooled cycle. The maximum electrical efficiency for steam-cooled cycle with a TIT of 1260°C is 51.3%, only 0.7 percentage points higher than that for the air-cooled cycle. The increase of the pressure ratio or TIT increases the advantage of the steam-cooled cycle over the air-cooled cycle in the electrical efficiency. Unlike the air-cooled PEvGT cycle, the steam-cooled PEvGT cycle with TIT's of 1371 and 1482°C provides more power output initially as the pressure ratio increases. The maximum power outputs for TIT's of 1371 and 1482°C are 93 and 106 MW at pressure ratios of 23 and 28, respectively.

Bartlett and Westermark [5] studied the performance of the PEvGT cycle and published the results of the air-cooled PEvGT cycle with a TIT of 1350ºC, which is consistent with the current calculation if the same operation conditions and similar assumptions are employed. Note that the pressure loss for the recuperative heat exchanger used to heat up the humid air is assumed to be 6% of the total pressure (2.1 bar at the pressure ratio of 35) in Bartlett and Westermark's study while the pressure loss for the humidification process is 2.7 bar for the results shown in Figure 5. Therefore, the efficiencies in Figure 5 are slightly lower than those from Bartlett and Westermark's study. The model for the steam-cooled PEvGT cycle is not directly verified because the performance data of the steam-cooled PEvGT cycle is not available in the literature. The assumptions and calculation methods for the steam-cooled PEvGT cycle are consistent with those for the air-cooled PEvGT cycle; thus, the steam-cooled model is indirectly verified through the calculation results of the air-cooled model.

Figure 6 displays three solid curves for the steam-cooled combined STIG cycle and three dotted curves for the air-cooled combined STIG cycle. As the TIT increases from 1260 to 1482°C for the air-cooled combined STIG cycle, the power output increases ~40 MW and the electrical efficiency gains 2.5 percentage points at a turbine pressure ratio of 16. These trends are in line with the other two HGT cycles. The increase of the pressure ratio reduces the power output but initially increases the efficiency for the air-cooled combined STIG cycle. The optimal pressure ratio for the maximum efficiency slightly increases with an increase in the TIT's. The optimal efficiencies for the TIT's between 1260 and 1482°C occur at a pressure ratio between 22 and 25.

The combined steam-cooled cycle has advantages over the combined air-cooled cycle in the electrical efficiency. The maximum electrical efficiency for steam-cooled cycle with a TIT of 1482°C is 54.4%, 1 percentage point higher than that for the air-cooled cycle. However, the steam-cooled combined STIG cycle does not always produce more power output than the air-cooled combined STIG cycle. The steam-cooled cycle has more power output than the air-cooled cycle only at high-pressure ratios.

The electrical efficiency of a HGT cycle strongly depends on the cooling flow rate for turbine stators and rotors. Figure 7 shows the cooling flow rate and temperature vs. the pressure ratio for air and steam-cooled combined STIG cycles. The cooling air flow rate increases with an increase in the pressure ratio mainly because the temperature of the cooling air increases with an increase in the pressure ratio. In contrast, the cooling steam flow rate decreases with an increase in the pressure primarily because the temperature of the cooling steam decreases with an increase in the pressure ratio. The cooling flow rate for the steam-cooled cycle is 1/2-1/3 that for the air-cooled cycle because the specific heat for steam is roughly twice that for air and because the temperature for the cooling steam is lower than that for the cooling air at the pressure ratio of 20 or greater. As a result, the steam-cooled cycle has a higher electrical efficiency than the air-cooled cycle does.

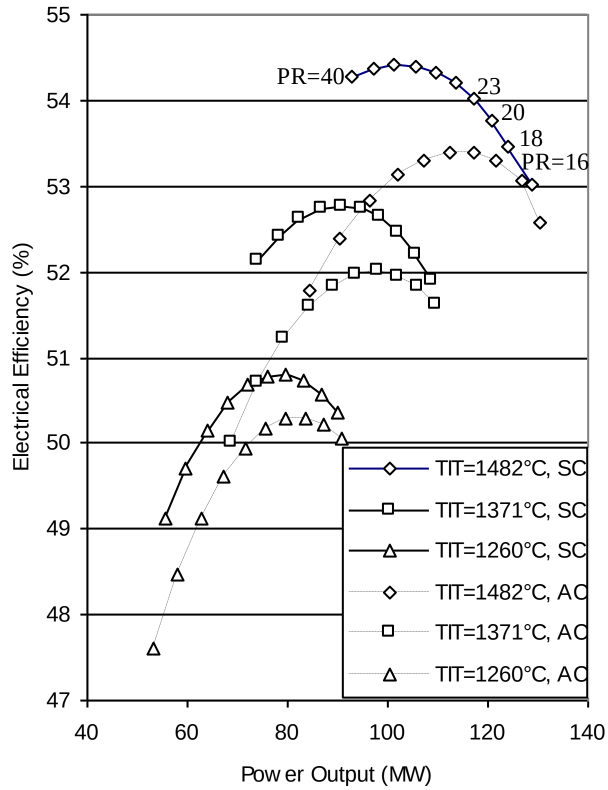

Figure 6. Electrical efficiencies and power outputs of steam and air-cooled combined STIG cycles.

The performance curves calculated in Figure 6 are based on a steam pressure of 100 bar (1450 psi) in the inlet of the steam turbine. Figure 8 shows the efficiencies at various steam turbine inlet pressures and pressure ratios for the air-cooled combined STIG at a TIT of 1482°C. The efficiency at a steam turbine inlet pressure of 100 bar is at or near the maximum for the pressure ratios ranging from 16 to 40. Thus, an inlet pressure of 100 bar is set for calculating the performance curves of the air-cooled and steam-cooled combined STIG cycles.

Many gas turbines for the STIG cycle are commercially available [3,4] but the pressure loss associated with steam injection into the combustor is significant for many of these turbines. In general, the gas turbines were originally built for a simple gas turbine cycle and then modified for the STIG cycle. Due to the limitations on the existing turbine design for the simple cycle, the modification generally may result in a significant pressure loss for injecting steam into the combustion chamber, higher than that assumed for calculating the performance curves in Figures 4-8. The pressure losses assumed in Figures 4-8 are based on the specially designed gas turbines for the three HGT cycles, resulting in lower pressure losses than those for gas turbines with retrofitted steam injection ports. This study also determined the sensitivity of the pressure loss on the performances of the STIG and combined STIG cycles such that the results from this study can be applied to various scenarios. The calculation result shows that each 6.9-bar (100-psi) of the pressure loss results in a reduction of 0.39 percentage points in the electrical efficiency for the steam-cooled combined STIG and 0.19 percentage points for the steam-cooled STIG cycle.

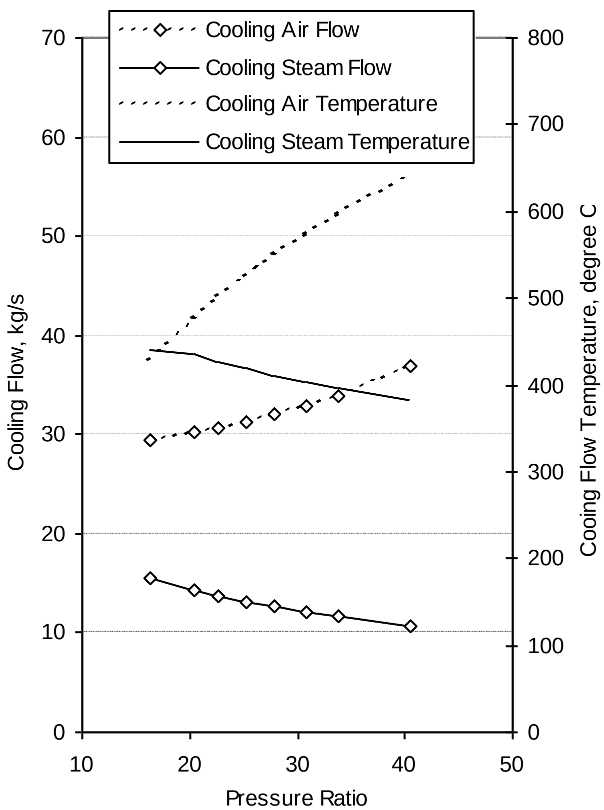

Figure 7. Cooling flow vs. pressure ratio for combined STIG cycles at a TIT of 1482ºC

Table 5. Maximum efficiency for HGT cycles at TIT of 1482°C

	Coolant	Maximum Efficiency	Pressure Ratio
STIG	Steam	53.5%	40
	Air	52.1%	28
PEvGT	Steam	54.6%	40
	Air	52.9%	31
Combined STIG	Steam	54.4%	34
	Air	53.4%	25

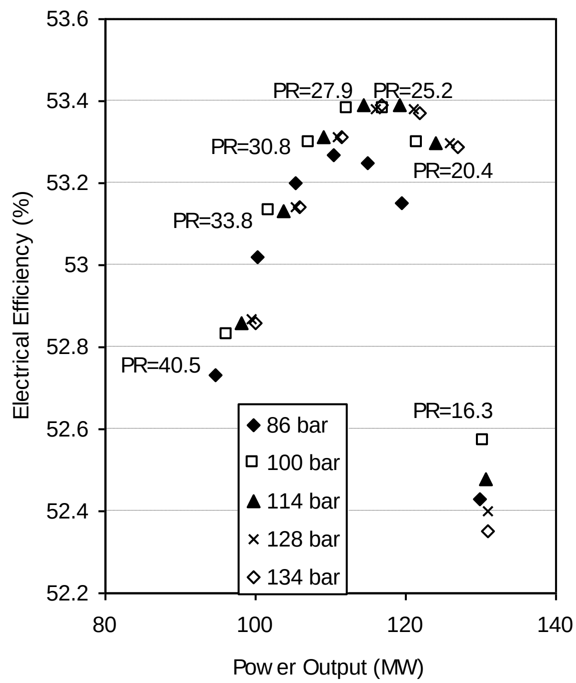

Fig. 8. Performance of combined STIG cycle as a function of steam turbine inlet pressure and turbine pressure ratio.

Of all the HGT cycles in this study, the steam-cooled PEvGT cycle has the highest efficiency (54.6%). However, the efficiency of the steam-cooled PEvGT cycle is only slightly better than that of the steam-cooled combined STIG cycle. The maximum efficiency for the steam-cooled PEvGT is 0.2 percentage points higher than that for the steam-cooled combined STIG and 1.1 percentage points higher than the steam-cooled STIG. Of the three air-cooled HGT cycles in this study, the combined STIG has the highest efficiency. The maximum electrical efficiency for the air-cooled combined STIG is 53.4%, 0.5 percentage points higher than that for the air-cooled PEvGT cycle and 1.3 percentage points higher than that for the air-cooled STIG cycle. The pressure ratio for the combined STIG at the maximum efficiency is smaller than those for the other two HGT cycles. The decrease of the pressure ratio for a turbine decreases the size and cost of the turbine. The maximum efficiencies for these three HGT cycles with steam cooling are 1-1.7 percentage points higher than those with air cooling.

A high humidity level in the humid air entering combustor characterizes the HGT cycles and may result in combustion instability [17]. This humidity levels for the steam-cooled HGT cycles are much lower than those for the air-cooled HGT cycles because the steam-cooled cycles use a portion of the steam for blade cooling, resulting in less steam injected into the combustor. For example, the mole fraction of the water vapor for the steam-cooled STIG cycle is 0.17 versus 0.34 for the air-cooled STIG cycle. Such a reduction in the humidity level may significantly improve combustion stability.

The HGT cycles in general consume a lot of water when a water recovery system is not employed. If the water source is limited for the HGT cycles, it may become necessary to add a water recovery system to recover water vapor from the flue gas. Therefore, some researchers studied water recovery systems for the HGT cycles. These water recovery systems may include a direct contact heat exchanger to reduce the temperature of the flue gas below its dew point such that some water can be condensed out of the flue gas [7]. Due to the limited space of the paper, this study focuses only on the HGT cycles without water recovery.

CONCLUSION

In this study, three representative HGT cycles have been evaluated with open-loop steam and air film cooling. The steam-cooled cycles provide advantages over the air-cooled cycles in the electrical efficiency, power output, and combustion stability. The open-loop steam film cooling improves the electrical efficiency by 1.4 percentage points for the STIG cycle, by 1.7 percentage points for the PEvGT cycle, and by approximately 1 percentage point for the combined STIG cycle. The steam film cooling in general increases the power output. In addition, the steam film cooling reduces the water content of the humid air entering the combustor from 0.34 to 0.17 for the STIG and combined STIG cycles, leading to significantly improved combustion stability. This study focuses the open-loop steam film cooling, instead of the closed loop convective steam cooling, because of the simplicity of the open-loop steam cooling.

The pressure loss associated with steam injection into the combustor may be quite significant for many commercially available STIG gas turbines that are not originally designed for steam injection. This pressure loss can be significantly reduced if a gas turbine is specially designed for steam injection. Therefore, it is important to understand the effect of the pressure loss on the performance of a gas turbine. The sensitivity study shows that each 6.9 bar of the pressure loss results in a decrease of 0.19 percentage points in the electrical efficiency for the steam-cooled STIG cycle and of 0.39 percentage points for the steam-cooled combined STIG cycle. Thus, designing an efficient STIG cycle requires minimizing the pressure loss.

The maximum electrical efficiency for the steam-cooled PEvGT is very close to that for the steam-cooled combined STIG. The maximum efficiency for the steam-cooled PEvGT is 0.2 percentage points higher than that for the steam-cooled combined STIG and 1.1 percentage points higher than that for the steam-cooled STIG cycle. Although the steam-cooled PEvGT cycle is more efficient than the steam-cooled combined STIG cycle, the optimal pressure ratio for the steam-cooled PEvGT cycle is higher than that for the combined STIG cycle. The increase of the pressure ratio for a gas turbine increases the size and cost of the gas turbine.

NOMENCLATURE

AC	= Air cooling
ARC	= Ratio of the surface area of the cooled blade wall and the cross-sectional area of the gas flow
CC	= Combined cycle
CF	= Correction factor for thermal barrier coating
$C_{p, c}$	= Specific heat of coolant
$C_{p, g}$	= Specific heat of gas
Econ	= Economizer for HRSG
EGT	= Evaporative gas turbine
Evap	= Evaporator
HRSG	= Heat recovery steam generator
HGT	= Humidified gas turbine
PEvGT	= Part-flow evaporative gas turbine
PR	= Pressure ratio
SC	= Steam cooling
SH	= Superheater
STIG	= Steam-injected gas turbine
TIT	= Turbine inlet temperature
T_{blade}	= Blade surface temperature
$T_{coolant}$	= Coolant temperature
T_{gas}	= Hot gas temperature
β	= Exponent of cooling effectiveness equation
φ	= Cooling effectiveness
φ_{∞}	= Maximum cooling effectiveness
n_c	= Mole flow rate of coolant
n_{gas}	= Mole flow rate of gas

ACKNOWLEDGMENTS

The author would like to thank GE Global Research for permission to publish this study.

DISCLAIMER

The data cited in this paper are obtained from trade publications and commercially available heat balance simulation tools that are listed in the references for the sole purpose of demonstrating key principles and order-of-magnitude estimates. As such they do not represent an actual plant performance of any vintage, past, present, or future that is offered and/or guaranteed by GE.

REFERENCES

[1] Jonsson, M., and Yan, J., 2005, “Humidified Gas Turbines—A Review of Proposed and Implemented Cycles,” Energy, 30, pp. 1013–1078.

[2] Bhargava, R. K., Bianchi, M., Campanari, S., De Pascale, A., Negri di Montenegro, G., and Peretto, A., 2008, “High Efficiency Gas Turbine Based Power Cycles – A Study of the Most Promising Solutions: Part 1 - A Review of the Technology”, ASME Paper No. GT2008-51275.

[3] Jones, J. L., Chang, C-N, Digumarthi, R. V., and Conlon, W. M., 1985, “Design and Construction of the First Commercial Cheng Cycle Series 7 Cogeneration Plant,” International Gas

Turbine Symposium and Exposition, Beijing, China, 85-IGT-122.
[4] Badeer, G. H., 2000, “GE Aeroderivative Gas Turbines – Design and Operating Features,” GER-3695E, GE Power Systems.
[5] Bartlett, M. A. and Westermark, M. O., 2005, “A Study of Humidified Gas Turbines for Short-Term Realization in Midsized Power Generation—Part I: Nonintercooled Cycle Analysis,” ASME J. Eng. Gas Turbines Power, Vol. 127, pp. 91–99.
[6] Westermark, M., 1996, ‘‘Method and Device for Generation of Mechanical Work and, if Desired, Heat in an Evaporative Gas Turbine Process,’’ International Patent Application No. PCT/SE96/00936.
[7] Higuchi, S., Koganezawa, T., Horiuchi, Y., Araki, H., Shibata T., and Marushima, S., 2008, “Test Results from the Advanced Humid Air Turbine System Pilot Plant - Part 1: Overall Performance,” Proc. of ASME Turbo Expo, Berlin Germany, GT2008-51072.
[8]Araki, H., Higuchi, S., Marushima, S. and Hatamiya, S., 2005, “Design Study of a Humidification Tower for the Advanced Humid Air Turbine System,” ASME 2005-GT-68671.
[9] Wang B., Zhang S., and Xiao Y., 2007, “Steady-State Off-Design Performance of Humid Air Turbine Cycle,” ASME 2007-GT-27350.
[10] Bartlett, M., 2002, “Developing Humidified Gas Turbine Cycles,” Ph.D. thesis, Royal Institute of Technology, Stockholm, Sweden.
[11] Bhargava, R. K., Bianchi, M., Campanari, S., De Pascale A., Negri di Montenegro, G., Peretto A., 2008, ”High Efficiency Gas Turbine Based Power Cycles -- A Study of the Most Promising Solutions: Part 2 -- A Parametric Performance Evaluation,” ASME-2008-GT-51277.
[12] Reale, M. J., 2004, “New High Efficiency Simple Cycle Gas Turbine – GE’s LMS100™”, GER-4222A (06/04).
[13] Frutschi, H. U., and Plancherel, A., 1988, ‘‘Comparison of Combined Cycle With Steam Injection and Evaporation Cycles,’’ Proc. 2nd Sym. on Turbomachinery, Combined-Cycle Technologies and Cogeneration, IGTI, Vol. 3, pp. 137–145.
[14] Horlock, J. H., 2003, *Advanced Gas Turbine Cycles*, Elsevier Science, Oxford, UK.
[15] Holland, M.J. and Thake, T.F., 1980, “Rotor blade cooling in high pressure turbines, AiAA J. Aircraft 17(6), 412-418.
[16] Elmasri, M. A. and F. Pourkey, 1986, "Prediction of Cooling Flow Requirements for Advanced Utility Gas Turbines – Part 1: Analysis and scaling of the Effectiveness Curve," ASME 86-WA/HT-43.
[17] Kuroki, H., Shibata, T., Koganezawa, T., Kizuka, N., Hatamiya, S., and Marushima, S., 2006, “Development of Elemental Technologies for Advanced Humid Air Turbine System,” ASME Paper GT2006-90643.